Theoretical multiconfiguration Dirac-Fock method study on the x-ray spectra of multiply ionized heavy atoms: The structure of the $K\alpha L^n$ lines

Marek Polasik
Institute of Physics, Nicholas Copernicus University, PL-87-100 Toruń, ul. Grudziądzka 5, Poland
(Received 18 March 1988; revised manuscript received 21 June 1988)

Relativistic multiconfiguration Dirac-Fock (MCDF) calculations in the average-level (MCDF-AL) version with the inclusion of the transverse (Breit) interaction, self-energy, and vacuum polarization corrections have been carried out for molybdenum, palladium, lanthanum, and holmium to elucidate the structure of the $K\alpha L^n$ lines in their x-ray spectra. The examination of the effect of removing electrons from M shell on the principal $K\alpha(K\alpha L^0)$ lines indicates that the most significant is the effect of removing $3p$ and then $3s$ subshells and that the effect of additional holes strongly increases with the atomic number. Detailed calculations have been performed on palladium to shed light on the structure of the $K\alpha L^n$ satellite lines of its x-ray spectrum, which is the first systematic theoretical study on the structure of these lines of a heavy atom. It has been found that in all cases the "average" positions of the groups of lines corresponding to the transitions of the type $1s^{-1}2p^{-n}\rightarrow 2p^{-(n+1)}$ obtained in the present work are very close to the recently measured experimental positions of appropriate $K\alpha L^n$ satellite lines. On the other hand, the structure of the satellite lines has been shown to be much more complex than can be observed experimentally. The results of this work can be used to construct different theoretical $K\alpha L^n$ spectra for palladium, satisfactorily reproducing the shape of various experimental spectra generated by different inducing projectiles.

I. INTRODUCTION

$K\alpha$ lines in the x-ray spectra are the result of transitions between an atomic ion state having at least one vacancy in $1s$ subshell and a state in which an electron from $2p$ subshell has filled this vacancy. If a neutral atom is in a closed-shell state and only one electron from $1s$ subshell has been removed, only two transitions of different energies are possible. In the case of the first transition, which corresponds to larger energy transfer, the total angular momentum j of the electrons in $2p$ subshell after transition is equal to $\frac{3}{2}$, while in the case of the second one it equals $\frac{1}{2}$. These two cases are reflected in x-ray spectra as lines $K\alpha_1$ and $K\alpha_2$, respectively [see Fig. 1(a)]. A transition of this type is usually denoted as $1s^{-1}\rightarrow 2p^{-1}$.

Generally if one removes one $1s$ electron from an atom in an open-shell state or more electrons, only one of them being $1s$, from an atom in an arbitrary state, the initial states have more than one open subshell. Therefore many configuration state functions (see Sec. II) differing in their total angular momentum J are possible for a certain configuration and, moreover, there are usually many different configuration state functions for a certain J. To describe particular initial and final states it is usually necessary to take a linear combination of the configuration state functions of a certain J (i.e., to apply an intermediate coupling[1]). All this implies transitions between large numbers of initial and final states. Because the states under consideration obviously differ in energy, there are no single lines $K\alpha_1$ and $K\alpha_2$, but either two groups of lines or even completely scattered lines. The groups of lines corresponding to transitions from initial states having one hole in the K shell and n holes in the L shell are the satellite $K\alpha$ lines[2,3] and are labeled by $K\alpha_1L^n$ and $K\alpha_2L^n$.

In the case of light elements (atomic number Z less than 20) the energy shift (the distance between the consecutive satellites) caused by introducing an additional hole in the L shell is remarkable (of order 0.5 hartree), while the separation between the $K\alpha_1L^0$ and $K\alpha_2L^0$ lines is small. It can be observed, however, that owing to the relativistic effects the distance between the $K\alpha_1L^0$ and $K\alpha_2L^0$ lines strongly increases with Z, while the increase of distance of the satellite lines is comparatively small. Therefore for heavy elements ($Z>40$) the distance between $K\alpha_1L^0$ and $K\alpha_2L^0$ lines becomes greater than that between the satellite lines, which implies the $K\alpha_2L^n$ satellites to be located between the $K\alpha_2L^0$ and $K\alpha_1L^0$ lines.[4] On the other hand, the natural linewidth is in the whole Z range less than the separation between the consecutive $K\alpha L^n$ satellites which, when high-resolution spectrometers are available, enables resolving the gross structure of the spectra.

Generally, the structure of $K\alpha$ x-ray spectrum depends both on the kind of the inducing particles and the Z value of the element under study.[5] In the case of molybdenum, for instance, generating the spectrum by 28-MeV ^{4}He ions leads practically to principle lines only.[4] On the contrary, acting with heavy 112-MeV ^{16}O ions results in strong $K\alpha L^n$ satellite lines,[4] because it is very likely that L-shell vacancies will appear apart from the K-shell vacancy.

The theory of relativistic atomic structure including the effects of quantum electrodynamics (QED) have been

well established in the literature. Recently an exhaustive review on these subjects for the atomic inner shells has been published.[3]

Several theoretical calculations on the x-ray spectra have been performed to assign the satellite lines.[3,4,6–16] Recently Kuhn and Scott[13] and Scott[14] have made an attempt to the theoretical assignment of the $K\alpha$ satellite lines for medium-Z elements ($19<Z<32$). However, their calculations were carried out in the nonrelativistic single-configuration Hartree-Fock scheme

In the case of heavy elements the relativistic effects are essential in the interpretation of the spectra. The number of such relativistic calculations is, however, small. The extensive multiconfiguration Dirac-Fock (MCDF) and configuration-interaction (CI) studies including the transverse interaction and QED corrections were carried out by Grant[12] on the satellite structure in the $K\beta$ x-ray spectrum of argon. Recently for heavy elements Dirac-Fock calculations of L x-ray transition energies have been performed by Uchal *et al.*[15].

In the present study MCDF calculations have been carried out on the $K\alpha L^n$ x-ray lines of molybdenum, palladium, lanthanum, and holmium with the use of Grant's program package.[17,18] This program enables one to carry out relativistic calculations with the inclusion of the transverse (Breit) interaction and QED (self-energy, and vacuum polarization) corrections, which is thought to be essential in the x-ray transitions in heavy elements.[3,19]

II. THEORETICAL BACKGROUND

The computational method used in the present study has been described in detail in many papers.[12,17–22] However, for the sake of clarity, some basic ideas are summarized here.

Within the MCDF scheme the effective Hamiltonian for an N-electron system is to be expressed by

$$H=\sum_{i=1}^{N} h_D(i)+\sum_{i<j}^{N} C_{ij} \ , \tag{1}$$

where $h_D(i)$ is the Dirac operator for ith electron,

$$h_D(i)=c\boldsymbol{\alpha}\cdot\mathbf{p}_i+(\beta-1)c^2+V_{\rm nuc}(r_i) \ . \tag{2}$$

In Eq. (2) c is the velocity of light; α_x, α_y, α_z, and β are fourth-order Dirac matrices: $\mathbf{p}_i$ is the momentum; and $V_{\rm nuc}(r_i)$ is the potential due to the nucleus which for a point nucleus has the form $V_{\rm nuc}(r_i)=-Z/r_i$.

The terms C_{ij} in Eq. (1) account for electron-electron interactions and come from one-photon exchange process. Each C_{ij} can be expressed[20] by

$$C_{ij}=1/r_{ij}+T(r_{ij}) \ , \tag{3}$$

where $1/r_{ij}$ is the Coulomb interaction operator (due to longitudinally polarized photons) and $T(r_{ij})$ is the transverse Breit operator (due to transversely polarized photons),

$$T(r_{ij})=-\frac{\boldsymbol{\alpha}_i\cdot\boldsymbol{\alpha}_j}{r_{ij}}+(\boldsymbol{\alpha}_i\cdot\boldsymbol{\nabla}_i)(\boldsymbol{\alpha}_j\cdot\boldsymbol{\nabla}_j)\frac{\cos(\omega r_{ij})-1}{\omega^2 r_{ij}} \ . \tag{4}$$

When the wave number of the photon being transferred, ω, is small, $T(r_{ij})$ reduces to the well-known Breit interaction $B(r_{ij})$,

$$B(r_{ij})=-\frac{1}{2r_{ij}}\left[\boldsymbol{\alpha}_i\cdot\boldsymbol{\alpha}_j+\frac{(\boldsymbol{\alpha}_i\cdot\mathbf{r}_{ij})(\boldsymbol{\alpha}_j\cdot\mathbf{r}_{ij})}{r_{ij}^2}\right] .$$

In the MCDF method an atomic state function (ASF) with the total angular momentum J and parity p is assumed in the multiconfigurational form[12,17]

$$\Psi_s(J^p)=\sum_{m=1}^{N_c} c_m(s)\Phi(\gamma_m J^p) \ , \tag{5}$$

where s numbers the states; $\Phi(\gamma_m J^p)$ are configuration state functions (CSF), i.e., the antisymmetrized products of one-electron spinors of specified angular symmetry labeled by J and overall parity p; N_c is the number of CSF's included in the expansion; $c_m(s)$ are the configuration mixing coefficients for state s; and γ_m represents all information required to uniquely define a certain CSF, i.e., orbital occupation numbers, values of j of all the subshells, the way they are coupled, and seniority numbers.

Actually, in solving the eigenproblem for such a Hamiltonian the transverse (Breit) interaction (4) is neglected. The corresponding energy contribution is added as a first-order perturbation correction after self-consistence is achieved.[18]

Applying the variational principle to the energy functional with such a defined Hamiltonian yields integrodifferential equations for the orbitals, which contain also the mixing coefficients $c_m(s)$ as parameters. In practice a trial set of orbitals is chosen to form the Hamiltonian matrix which after diagonalization gives the set of coefficients, which in turn can be inserted into the integrodifferential equations mentioned above to give "improved" orbitals. The cycle is repeated until convergence is achieved. Such a scheme is called the optimal level version of MCDF calculation[12,17] (MCDF-OL).

The preceding iterative cycle is omitted in the average level version of MCDF (Refs. 12 and 17) (MCDF-AL) calculations. In this case the energy functional averaged over all the initial and final states is to be minimized and therefore orbitals have to be calculated only in the first step. In the second step the coefficients $c_m(s)$ corresponding to the orbitals found in the first step are determined by diagonalizing the matrix of the Hamiltonian in the space of the CSF. It is evident that for each particular state such orbitals yield higher energy (the effect of relaxation) than those obtained from MCDF-OL calculations for each state. However, usually all energy levels are shifted by approximately the same extent (see Sec. III.)

There are two reasons for performing MCDF-AL calculations. First they require less computational time than MCDF-OL calculations, as the latter imply repeating the whole procedure for each state, and even for a given state they are more laborious than MCDF-AL. Second and much more important is the fact that because the orbitals obtained in such a way are common for all the states considered, applying the MCDF-AL version is especially useful for performing calculations of the proba-

bilities and oscillator strengths of the transitions.

Apart from the transverse (Breit) interaction two types of energy corrections are significant in the case of heavy atoms, namely, the self-energy (E_{SE}) and vacuum polarization (E_{VP}) corrections.[18,21] The corresponding expressions are given by (6) and (7), respectively,

$$E_{SE}=(Z^4\alpha^3/\pi)\sum_a F_a(Z\alpha)q_a/n_a^3 , \quad (6)$$

$$E_{VP}=\sum_a q_a\int_0^\infty [P_a^2(r)+Q_a^2(r)]V_{VP}(r)dr , \quad (7)$$

where the sums run over all occupied orbitals, α is the fine-structure constant, q_a is the occupation number of the orbital, n_a is its principle quantum number, $P_a(r)$ and $Q_a(r)$ are large and small radial components of Dirac orbital, and V_{VP} is the vacuum polarization potential described by Fullerton and Rinker.[23] The values of $F_a(Z\alpha)$ are calculated using an interpolation procedure of McKenzie, Grant, and Norrington[18] on the basis of the exact values obtained for $1s$, $2s$, and $2p$ orbitals by Mohr.[24]

The formulas for the transition matrix elements, spontaneous emission probabilities, and oscillator strengths can be found in the work of Grant.[22]

III. RESULTS AND DISCUSSION

The capability of the MCDF method with the inclusion of the transverse (Breit) interaction, self-energy, and vacuum polarization corrections in the calculations of x-ray transitions energies is well known.[3,19] In the MCDF-AL calculations of the transition energies (see Sec. II) the orbitals are common for all the simultaneously considered initial and final states. The test calculations which examine how important is the effect of relaxation (and the role of the particular contributions) on the states and transition energies have been performed for Pd^+ (see Table I). Because in the present study the electron correlation has not been taken into account the MCDF-OL calculations for the states displayed in Table I are in fact one-configuration Dirac-Fock ones (for the explanation of the abbreviations see the caption of Table I).

As shown, the MCDF-AL state energies corrected by adding TB (transverse Breit), SE, and VP corrections [denoted as MCDF(T)-AL] are higher (by about 0.1 hartree) than those of the DF state energies corrected by adding TB, SE, and VP corrections [denoted as DF(T)], while the effect of relaxation on the $K\alpha_1L^0$ and $K\alpha_2L^0$ transition energies is very small (of order of 0.03 hartree). The agreement between the $K\alpha_1L^0$ and $K\alpha_2L^0$ transition energies calculated in MCDF(T)-AL scheme and their experimental counterparts is very good. This means that the MCDF(T)-AL scheme is adequate to carry out calculations for the $K\alpha$ x-ray transitions. It can be observed that the transverse (Breit) interaction and next the self-energy correction are important for the state and transition energies, while the vacuum polarization contribution is remarkably smaller. Moreover, the influence of a finite-size nucleus on both states and transition energies is very small.

In this section we present the results of calculations, which have been carried out in the relativistic MCDF-AL scheme with the use of the Grant program package.[17,18] First the effect of removing M-shell electrons on the principal $K\alpha$ ($K\alpha L^0$) lines for molybdenum, palladium, lanthanum, and holmium is analyzed. Finally, the results of detailed calculations of the $K\alpha L^n$ satellite lines are presented. The knowledge of the structure of these lines will enable the construction of different theoretical spectra for palladium.

A. Effect of removing electrons from M shells on the $K\alpha L^0$ lines

One of the salient features of heavy-ion-induced $K\alpha$ x-ray spectra is the high probability of multiple ionization of N, M, and L shell.[4] It was therefore thought worthwhile to examine the influence of additional holes

TABLE I. Effect of relaxation and role of the particular contributions to the states and transition energies for Pd^+ (in hartrees). The following methods are used: DF, one-configuration Dirac-Fock; TB, transverse Briet correction; SE, self-energy correction; VP, vacuum polarization correction; DF(T), DF corrected by adding TB, SE, and VP corrections; MCDF(T)-AL, MCDF-AL version (see Sec. II) corrected by adding TB, SE, and VP corrections.

	States energies		Transition energies	
Method	$1s^12p^6$	$1s^22p^5$ $J=\frac{3}{2}$	$K\alpha_1L^0$	$K\alpha_2L^0$
DF	−4146.734	−4927.471	780.737	774.882
TB	+1.503	+3.112	−1.609	−1.518
SE	+1.368	+2.375	−1.007	−1.018
VP	−0.175	−0.305	+0.130	+0.130
DF(T)	−4144.038	−4922.289	778.251	772.477
MCDF(T)-AL	−4143.938	−4922.218	778.280	772.520
MCDF(T)-AL[a]	−4143.885	−4922.125	778.240	772.480
Expt.[b]			778.242	772.472

[a]Calculations assuming a finite-size nucleus (uniform distribution of nuclear charge).
[b]Bearden (Ref. 25).

in the M shell on the $K\alpha L^0$ transition energies.

The results of MCDF-AL and MCDF(T)-AL calculations are collected in Table II. In all cases all electrons from the subshell under consideration have been removed, as this does not lead to increasing of the number of possible transitions.

At first it should be noted that including transverse Breit interaction, self-energy, and vacuum polarization corrections [passing from MCDF-AL to MCDF(T)-AL] remarkably changes the shift for both $K\alpha_1 L^0$ and $K\alpha_2 L^0$ lines. Generally at both levels of calculations the shift of $K\alpha_1 L^0$ lines is significantly greater than that of $K\alpha_2 L^0$ lines. Only in the case of negative shifts is the situation the opposite.

As shown, the greater the atomic number, the greater the effect of additional holes on the transition energies. In the case of Mo^+, Pd^+, and La^{2+} the most significant effect is the effect of removing $3p$ and next $3s$ subshells, while removing the $3d$ subshell has a relatively small influence on the transition energies. On the contrary, in the case of Ho^{2+} the $3d$ holes also play a significant role.

It is very important to note that these effects are not additive. Consider, for example, the case of palladium. The sum of shifts after removing $3s$, $3p$, and $3d$ subshells is 2.221 hartree, while the shift after removing all these electrons simultaneously is 3.042 hartree. Therefore to better explain the influence of additional holes in the M shell on the $K\alpha L^0$ transition energies it is necessary to perform a detailed investigation in which any M-shell electrons and not whole subshells will be removed (the $K\alpha L^0 M^r$ lines for $r=1,2,3,\ldots$).

Preliminary calculations for the simplest case of the $K\alpha L^0 M^r$ lines have been recently performed on palladium. In this case ($K\alpha L^0 M^1$ lines) we have three possible types of transitions, $(1s3s)^{-1}\rightarrow(2p3s)^{-1}$, $(1s3p)^{-1}\rightarrow(2p3p)^{-1}$, and $(1s3d)^{-1}\rightarrow(2p3d)^{-1}$. For each type of transition two groups of lines ($K\alpha_1 L^0 M^1$ and $K\alpha_2 L^0 M^1$) are observed. The relative "average" (see Sec. III B) positions of groups of lines $K\alpha_1 L^0 M^1$ with respect to $K\alpha_1 L^0 M^0$ and $K\alpha_2 L^0 M^1$ with respect to $K\alpha_2 L^0 M^0$ have been shown in Table III. The comparison of these relative positions with the values (from Table II) calculated per one electron displayed (in Table III) in the parentheses reveals that only for the type $(1s3s)^{-1}\rightarrow(2p3s)^{-1}$ a good agreement is observed while for two types of transitions [$(1s3p)^{-1}\rightarrow(2p3p)^{-1}$ and $(1s3d)^{-1}\rightarrow(2p3d)^{-1}$] the values are significantly different. These discrepancies confirm the great nonadditivity of these effects noted above. Moreover, the results presented in Table III corroborate my previous conclusion that removing $3p$ electron is more effective than the $3s$ or $3d$ electron in producing the $K\alpha L^0$ energy shift

TABLE II. Effect of removing all electrons from given subshells of the M shell on the $K\alpha L^0$ lines (in hartrees). The upper values correspond to $K\alpha_1 L^0$, while the lower values to $K\alpha_2 L^0$ transitions. The initial state configurations for the $K\alpha L^0 M^0$ transitions are

Mo^+, $1s^1 2s^2 2p^6 3s^2 2p^6 3d^{10} 4s^2 4p^6 4d^4_- 5s^2$;

Pd^+, $1s^1 2s^2 2p^6 3s^2 3p^6 3d^{10} 4s^2 4p^6 4d^{10}$;

La^{2+}, $1s^1 2s^2 2p^6 3s^2 3p^6 3d^{10} 4s^2 4p^6 4d^{10} 5s^2 5p^6 6s^2$;

Ho^{2+}, $1s^1 2s^2 2p^6 3s^2 3p^6 3d^{10} 4s^2 4p^6 4d^{10} 4f^{14} 5s^2 5p^2_- 6s^2$.

In the case of not fully occupied $4d$ and $5p$ subshells their parts corresponding to lower j in j-j coupling have been filled which gives the lowest energy. In this case $j=l-\frac{1}{2}$, which is indicated with the subscript "$-$".

Ion	Method	$3s$	$3p$	$3d$	$3s,3p$	$3s,3d$	$3p,3d$	$3s,3p,3d$
Mo^+	MCDF-AL	0.338	1.501	−0.146	1.939	0.331	1.940	2.555
($Z=42$)		0.314	1.423	−0.238	1.834	0.209	1.742	2.323
	MCDF(T)-AL	0.346	1.533	−0.180	1.983	0.307	1.943	2.570
		0.323	1.457	−0.271	1.882	0.187	1.750	2.344
Pd^+	MCDF-AL	0.423	1.811	−0.013	2.327	0.542	2.356	3.042
($Z=46$)		0.407	1.752	−0.059	2.247	0.472	2.217	2.872
	MCDF(T)-AL	0.437	1.861	−0.053	2.393	0.517	2.370	3.073
		0.422	1.803	−0.100	2.316	0.447	2.233	2.907
La^{2+}	MCDF-AL	0.651	2.688	0.280	3.457	1.100	3.624	4.585
($Z=57$)		0.610	2.537	0.150	3.255	0.911	3.282	4.176
	MCDF(T)-AL	0.681	2.793	0.190	3.595	1.040	3.646	4.643
		0.641	2.645	0.058	3.400	0.852	3.308	4.240
Ho^{2+}	MCDF-AL	1.079	4.058	1.285	5.229	2.505	5.904	7.241
($Z=67$)		0.974	3.711	0.943	4.768	2.040	5.147	6.351
	MCDF(T)-AL	1.137	4.254	1.149	5.489	2.430	5.974	7.378
		1.035	3.914	0.807	5.039	1.968	5.225	6.499

TABLE III. Influence of removing one electron from 3s, 3p, or 3d subshells (the "average" effect for $K\alpha_1 L^0 M^1$ and $K\alpha_2 L^0 M^1$ groups of lines) on the $K\alpha L^0$ energies for palladium (in hartrees) calculated at the MCDF(T)-AL level. In parentheses we display, for comparison, the values of effects per one electron obtained from Table II with the assumption that the shifts are proportional to the number of removed electrons.

Types of transitions	$K\alpha_1 L^0 M^1$	$K\alpha_2 L^0 M^1$
$(1s3s)^{-1} \rightarrow (2p3s)^{-1}$	0.211 (0.219)	0.209 (0.211)
$(1s3p)^{-1} \rightarrow (2p3p)^{-1}$	0.444 (0.310)	0.369 (0.300)
$(1s3d)^{-1} \rightarrow (2p3d)^{-1}$	0.042 (−0.001)	0.025 (−0.006)

(this has been already pointed out for xenon[3] and recently for molybdenum[4]). The reliable explanation of this fact seems to be difficult with the data available so far and therefore further detailed studies on the $K\alpha L^0 M^r$ lines are required.

B. Structure of the $K\alpha L^n$ spectrum of palladium

As pointed out in the Introduction, removing additional electrons from L shell results in appearing of the $K\alpha L^n$ satellite lines in the spectrum. To examine the influence of various types of additional L-shell holes on the structure of the $K\alpha L^n$ satellite lines, an extensive study has been carried out on palladium the ground state of which is a closed-shell state.

As has been shown MCDF(T)-AL scheme is proper to carry out calculations on the $K\alpha$ x-ray transitions. Moreover, at this level of calculation it is easy to obtain the probabilities of transitions between the states under consideration. Therefore all subsequent calculations have been performed at this level.

Let us first consider the "pure" $K\alpha L^n$ transitions, i.e., those in which there are no holes in shells higher than L. All the types of transitions considered can be classified into four groups, depending on the number of holes in the L shell in the initial state. These are $K\alpha L^0$ (principal lines), $K\alpha L^1$, $K\alpha L^2$, and $K\alpha L^3$. Schematic diagrams of transitions (transitions diagrams) for all these cases are presented in Figs. 1, 3, 5, and 6. In the cases when the number of possible transitions is too large, only the transitions of a remarkable intensity have been indicated in the diagrams.

As it has been pointed out in the Introduction, the correct description of the atomic state requires usually applying an intermediate coupling (i.e., mixing of configuration state functions of a certain J). The functions to be combined can be chosen either on the j-j or on the L-S basis. In Table IV the CI coefficients for those two bases for a sample case are presented. It can easily be noted that for the j-j basis each state consists nearly of one configuration while when the L-S basis is chosen the configuration state functions are always strongly mixed. Therefore the j-j coupling seems to be a good description of the energy levels and such a description is therefore employed in the transition diagrams.

Before discussing the obtained results in detail let us note that in several cases the same type of the transition diagram (see Fig. 1) corresponds to different types of satellite transitions. This is the case in which the corresponding initial states differ in the number of removed closed subshells (for example, the $(1s2p)^{-1} \rightarrow 2p^{-2}$ transition diagram for the $K\alpha L^1$ satellite is identical with that of $1s^{-1}2s^{-2}2p^{-1} \rightarrow (2s2p)^{-2}$ for the $K\alpha L^3$ satellite). In such cases the structures of the groups of lines are very similar though the absolute positions of the appropriate lines are shifted with respect to each other. It was therefore thought worthwhile to group spectra corresponding to a given type of transition diagram. To make the comparison easier, the energy axes have been shifted.

For the $K\alpha L^0$ type of transition in the case of the closed-shell atom (see Sec. I) only two lines are present, namely, $K\alpha_1 L^0$ and $K\alpha_2 L^0$. The transition diagram is shown in Fig. 1(a), and the corresponding values of transition energies, transition probabilities, and oscillator strengths are presented in Table V.

For the simplest $K\alpha L^1$ satellite the transitions can be either of the type $(1s2s)^{-1} \rightarrow (2s2p)^{-1}$ or

TABLE IV. Comparison of the CI eigenvectors for $2p^4$ configuration of Pd^{2+} in the j-j and L-S basis. The eigenvectors in the L-S basis were obtained by a unitary transformation of the eigenvectors in j-j basis.

		Eigenvectors				
Basis	J	1	2	3	4	5
j-j						
$2p^{\frac{3}{2}}\,2p^{\frac{3}{2}}$	2	0.9979	0.0000	0.0000	−0.0646	0.0000
$2p^{\frac{1}{2}}\,2p^{\frac{3}{2}}$	2	0.0646	0.0000	0.0000	0.9979	0.0000
$2p^{\frac{1}{2}}\,2p^{\frac{3}{2}}$	1	0.0000	0.0000	1.0000	0.0000	0.0000
$2p^{\frac{3}{2}}\,2p^{\frac{3}{2}}$	0	0.0000	0.9960	0.0000	0.0000	0.0893
$2p^{\frac{1}{2}}\,2p^{\frac{1}{2}}$	0	0.0000	−0.0893	0.0000	0.0000	0.9960
L-S						
$2p^4\,{}^3P$	2	0.8521	0.0000	0.0000	0.5234	0.0000
$2p^4\,{}^1D$	2	0.5234	0.0000	0.0000	−0.8521	0.0000
$2p^4\,{}^3P$	1	0.0000	0.0000	1.0000	0.0000	0.0000
$2p^4\,{}^3P$	0	0.0000	0.6479	0.0000	0.0000	−0.7617
$2p^4\,{}^1S$	0	0.0000	0.7617	0.0000	0.0000	0.6479

$(1s2p)^{-1}\rightarrow 2p^{-2}$. The transition diagrams are displayed in Figs. 1(b) and 1(c) and the theoretical "stick" spectra in Figs. 2(a) and 2(b). The numerical values are presented in Tables VI and VII. As shown, in the first case there are 6 states and 6 possible transitions, while in the second case there are 9 states and 14 transitions, of which 11 are of a remarkable intensity. However, in thees two cases we observe two groups of lines, the "average" positions of which are shifted (see Table IX) by about 2 hartree with respect to the $K\alpha L^0$ lines.

In the case of $K\alpha L^2$ we have three possible types of transitions, $1s^{-1}2s^{-2}\rightarrow 2s^{-2}2p^{-1}$, $1s^{-1}2p^{-2}\rightarrow 2p^{-3}$, and $(1s2s2p)^{-1}\rightarrow 2s^{-1}2p^{-2}$. The first one [see Fig. 1(a)] is the simplest case as far as the satellite lines are concerned as its structure is identical with the structure of the principal $K\alpha L^0$ transitions. The numerical values are collected in Table VIII. It can be observed (see Table IX) that the transition energy is by about 4 hartree higher than in the case of the principal lines, the shift being greater in the case of $K\alpha_1 L^2$, and the intensity of the lines increases by about 3%.

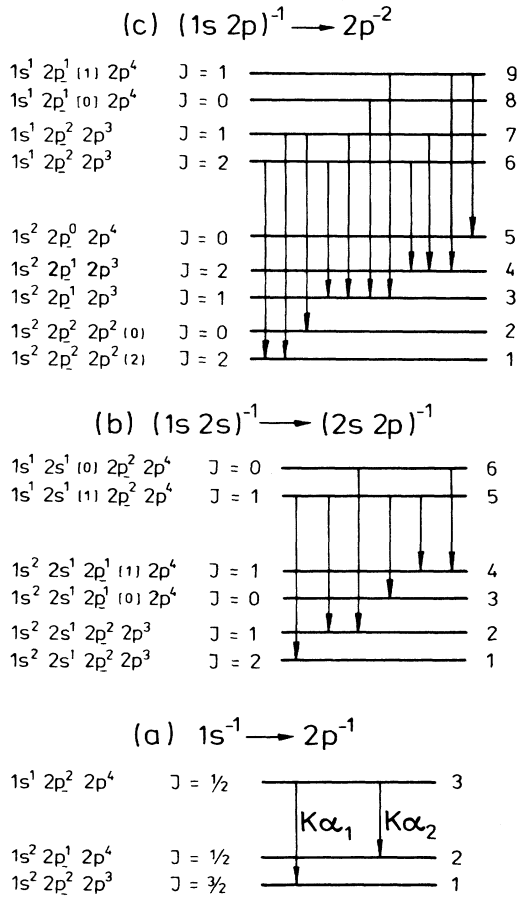

FIG. 1. Transition diagrams of the following types: (a) $1s^{-1}\rightarrow 2p^{-1}$ ($K\alpha L^0$ lines) and $1s^{-1}2s^{-2}\rightarrow 2s^{-2}2p^{-1}$ ($K\alpha L^2$ satellite); (b) $(1s2s)^{-1}\rightarrow(2s2p)^{-1}$ ($K\alpha L^1$); (c) $(1s2p)^{-1}\rightarrow 2p^{-2}$ ($K\alpha L^1$) and $1s^{-1}2s^{-2}2p^{-1}\rightarrow(2s2p)^{-2}$ ($K\alpha L^3$ satellite). All the transition diagrams refer to the j-j coupling. A "$-$" below the subshell symbol indicates that $j=l-\frac{1}{2}$; otherwise $j=l+\frac{1}{2}$. For the sake of clarity only those subshells whose occupation of which must be known for the unique description of the states are indicated; i.e., $1s$, $2p_-$, $2p$, and, in some cases, $2s$ subshells. For each state its total angular momentum J is indicated. When necessary, also the intermediate angular momentum is shown (the number in square brackets), as well as the angular momentum of the $2p$ subshell (the number in parentheses).

TABLE V. Calculated parameters of the principal $K\alpha$ lines of palladium. Transition $3\rightarrow 1$ corresponds to $K\alpha_1 L^0$ and $3\rightarrow 2$ to $K\alpha_2 L^0$ [see diagram in Fig. 1(a)]. In the case of the spontaneous transition probabilities and oscillator strength the upper values correspond to Coulomb gauge and the lower values to Babushkin gauge (in this and all subsequent tables). In this and all subsequent tables the numbers in square brackets signify powers of 10, e.g., $2.821[15]=2.821\times 10^{15}$.

Transition	Energy (hartrees)	Spont. trans. prob. per sec.	Oscillator strength
$3\rightarrow 1$	778.2801	4.125[15]	−0.1060
		4.185[15]	−0.1075
$3\rightarrow 2$	772.5197	2.185[15]	−0.1140
		2.216[15]	−0.1156

In the case of the $1s^{-1}2p^{-2}\rightarrow 2p^{-3}$ type of transition there are 13 states and 35 possible transitions, 21 being of a remarkable intensity [see Figs. 3(a) and 4(a)]. The most complex is the structure of the last transition type. There are 15 states and 47 transitions of which 29 are of a remarkable intensity [see Figs. 3(b) and 4(b)].

For $K\alpha L^3$ the transitions are of the type $1s^{-1}2s^{-2}2p^{-1}\rightarrow(2s2p)^{-2}$, $1s^{-1}2p^{-3}\rightarrow 2p^{-4}$, and $1s^{-1}2s^{-1}2p^{-2}\rightarrow 2s^{-1}2p^{-3}$. The first one has the same transition diagrams as the type $(1s2p)^{-1}\rightarrow 2p^{-2}$ of the $K\alpha L^1$ satellite [see Fig. 1(b)], and therefore for comparison the theoretical spectrum is shown in Fig. 2(c). As shown, the structure of the spectrum is similar to that corresponding to $K\alpha L^1$ satellite lines, while the transition energies (see Table IX) increase by about 4 hartree.

The second type (see Fig. 5) has 15 states and 35 possible transitions, of which 23 are of a remarkable intensity. The spectrum is shown in Fig. 7(a). For the last type (see Fig. 6) there are 26 states and 121 transitions, of which over 48 are intense. The stick spectrum is shown in Fig. 7(b).

In the last case it can be observed that the structure of the spectra is extremely complex. The distances between the neighboring lines become small, of order of 0.1 hartree, and the lines are more scattered than for previous types of transitions. Taking into account the natural linewidth,[27] which is of order of 0.3 hartree, it can easily be concluded that only two weakly structured bands would be observed experimentally, the resolution of which would clearly be impossible.

The above have presented only the structures of the particular types of transitions for each $K\alpha L^n$ satellite. In fact the situation is much more complex, because in the case of each satellite the groups of lines corresponding to different types of transitions strongly overlap. Moreover, we must not forget that the real spectrum will in general consist of all the groups of lines corresponding to

different $K\alpha L^n$ satellites, which in some cases also strongly overlap (see the absolute line positions in the stick spectra in Figs. 2, 4, and 7).

In Figs. 2, 4, and 7 are also indicated the recently measured[26] experimental positions of appropriate $K\alpha L^n$ satellite lines of palladium, together with their uncertainty intervals. As shown, in each case they are close to the "average" theoretical positions of the lines belonging to $K\alpha L^1$, $K\alpha L^2$, or $K\alpha L^3$ satellite. In fact, they are slightly shifted to the right. This is due to the fact that in the experimental spectra also the effect of M-shell vacancies occurs, which shifts the positions of the bands towards higher energies. On the other hand, it can be seen that the uncertainty intervals of the experimental positions of the $K\alpha L^n$ satellite lines are rather wide, and in some cases exceed the distance between the furthest theoretical

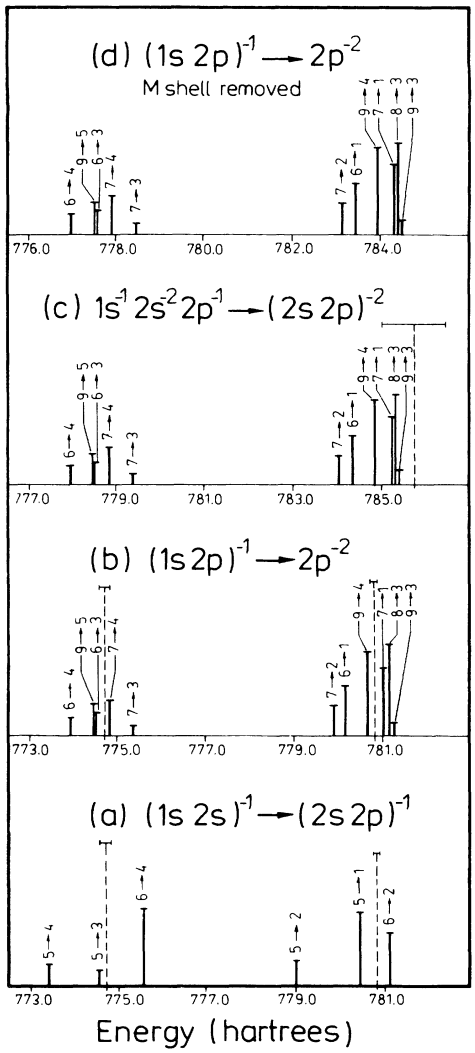

FIG. 2. Calculated positions (in hartrees) of the $K\alpha L^n$ satellite lines with their relative intensities, to the same scale, displayed in a stick spectrum (the Coulomb gauge was used). Transition types are (a) $K\alpha L^1$ in the case of $(1s2s)^{-1}\rightarrow(2s2p)^{-1}$; (b) $K\alpha L^1$ in the case of $(1s2p)^{-1}\rightarrow 2p^{-2}$; (c) $K\alpha L^3$ in the case of $1s^{-1}2s^{-2}2p^{-1}\rightarrow(2s2p)^{-2}$; (d) $K\alpha L^1$ in the case of $(1s2p)^{-1}\rightarrow 2p^{-2}$, with the M shell removed (influence of removing all electrons from the M shell on the satellite $K\alpha L^1$ lines). The recently measured (Ref. 26) experimental positions of the appropriate $K\alpha L^n$ satellite lines are shown as dotted lines.

TABLE VI. Calculations on the $K\alpha L^1$ satellite lines. The transition type is $(1s2s)^{-1}\rightarrow(2s2p)^{-1}$. For the transition diagram see Fig. 1(b).

Transition	Energy (hartrees)	Spont. trans. prob. per sec.	Oscillator strength
5→1	780.4552	3.494[15]	−0.1071
		3.457[15]	−0.1060
5→2	778.9720	1.196[15]	−0.0613
		1.183[15]	−0.0607
6→2	781.1181	2.719[15]	−0.0462
		2.686[15]	−0.0457
5→3	774.5673	7.389[14]	−0.1150
		7.318[14]	−0.1139
5→4	773.4353	9.809[14]	−0.0510
		9.717[14]	−0.0506
6→4	775.5815	3.686[15]	−0.0636
		3.646[15]	−0.0629

TABLE VII. Calculations on the $K\alpha L^1$ satellite lines. The transition type is $(1s2p)^{-1}\rightarrow(2p)^{-2}$ [see the transition diagram in Fig. 1(c)]. Only transitions probabilities of which are greater than 2×10^{14} have been listed. The number of all possible transitions is 14.

Transition	Energy (hartrees)	Spont. trans. prob. per sec.	Oscillator strength
6→1	780.1505	2.317[15]	−0.1185
		2.343[15]	−0.1198
7→1	781.0148	3.188[15]	−0.0976
		3.226[15]	−0.0988
7→2	779.8617	1.410[15]	−0.2164
		1.423[15]	−0.2185
6→3	774.4992	1.118[15]	−0.0967
		1.130[15]	−0.0977
7→3	775.3635	4.635[14]	−0.0240
		4.687[14]	−0.0243
8→3	781.1071	4.233[15]	−0.0720
		4.287[15]	−0.0729
9→3	781.1843	6.146[14]	−0.0313
		6.220[14]	−0.0317
6→4	773.9570	9.157[14]	−0.0476
		9.257[14]	−0.0481
7→4	774.8213	1.748[15]	−0.0544
		1.769[15]	−0.0550
9→4	780.6421	3.981[15]	−0.1220
		4.031[15]	−0.1235
9→5	774.4755	1.490[15]	−0.2320
		1.506[15]	−0.2344

TABLE VIII. Calculations on the $K\alpha L^2$ satellite lines. The transition type is $1s^{-1}2s^{-2} \rightarrow 2s^{-2}2p^{-1}$ [see diagram in Fig. 1(a)].

Transition	Energy (hartrees)	Spont. trans. prob. per sec.	Oscillator strength
3→1	782.4191	4.258[15]	−0.1083
		4.267[15]	−0.1085
3→2	776.4762	2.251[15]	−0.1162
		2.256[15]	−0.1165

lines belonging to a given group of lines.

A detailed comparison of the theoretical and experimental[26] positions of $K\alpha L^n$ satellite lines is presented in Table IX. The theoretical positions of the respective groups of lines have been calculated by taking the weighted averages of all the transitions energies corresponding to a given transition type, the weights being the transition probabilities multipied by the degeneracies of the initial states, which are $2J+1$.

An additional averaging taking into account different probabilities of creating appropriate types of initial configurations has been performed to obtain the theoretical "average $K\alpha L^n$" positions (see footnote h in Table IX) of the satellite lines.

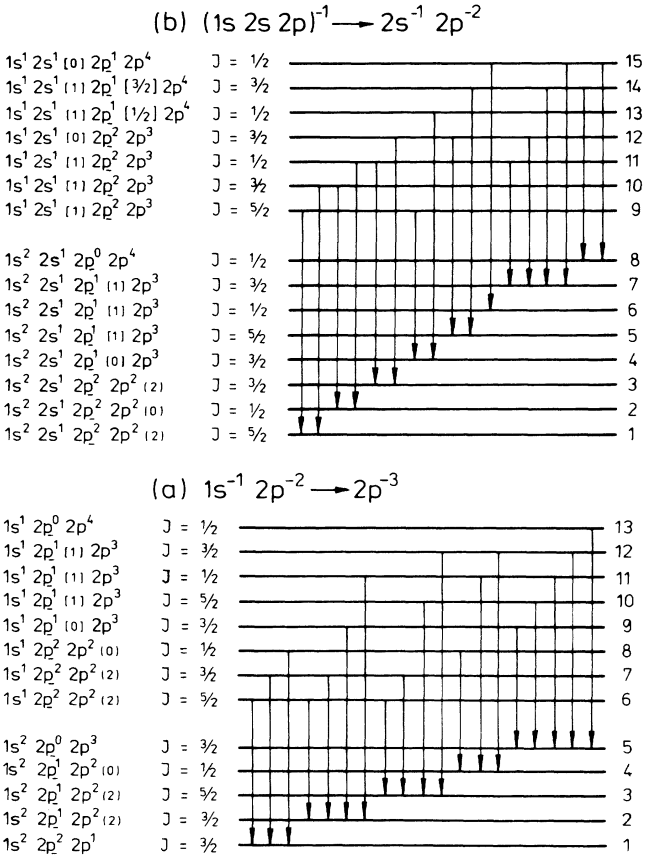

FIG. 3. Transition diagrams for $K\alpha L^2$ satellite lines of the types (a) $1s^{-1}2p^{-2} \rightarrow 2p^{-3}$, (b) $(1s2s2p)^{-1} \rightarrow 2s^{-1}2p^{-2}$.

Because in the theoretical calculations presented in Table IX the effect of removing electrons from the M shell has not been taken into account, for a better comparison of the theoretical and experimental values also the relative positions of each $K\alpha L^n$ satellite lines with respect to $K\alpha L^0$ lines have been given in which this effect is compensated. These values are in a much better agreement with experiment than the absolute positions of $K\alpha L^n$ satellite lines.

As shown, generally in each case the average theoretical relative positions of the groups of lines are rather close to the experimental positions of the appropriate $K\alpha L^n$ satellite lines. However, the average relative positions for the transitions from the states which contain $2s$ holes are in most cases significantly (even more than by the uncertainty of experimental values) shifted when compared with experiment. This means that the contributions of such transitions to certain $K\alpha L^n$ satellite lines are rather small which, on the other hand, is justified because due to the Coster-Kronig transitions[29] the $2s$ holes are rapidly filled, which greatly reduces the probability of radiative transitions from these states. This has been pointed out in several papers[6–8,13] dealing with atoms with small and medium Z.

In fact in all the cases the relative experimental positions of the $K\alpha L^n$ satellite lines (see Table IX) are closest to the average theoretical positions of the groups of lines corresponding to transitions of the type $1s^{-1}2p^{-n} \rightarrow 2p^{-(n+1)}$. Moreover, the discrepancies between theoretical relative positions of the groups of lines of the type $1s^{-1}2p^{-n} \rightarrow 2p^{-(n+1)}$ and their experimental counterparts are in all the cases much smaller than the uncertainty of experiment.

On the other hand, in most cases the theoretical "average $K\alpha L^n$" positions (see Table IX) are significantly more shifted when compared with experiment than the positions of the groups of lines of type $1s^{-1}2p^{-n} \rightarrow 2p^{-(n+1)}$. This indicates that the influence of the Coster-Kronig transitions may be very important and to get a high accuracy it is necessary to consider the quantitative effect of those transitions. It is worth noting that for "average $K\alpha L^n$" the $K\alpha_2/K\alpha_1$ probability ratio remarkably decreases with increasing n and always strongly decreases with increasing number of $2p$ holes.

In the preceding section the influence of removing subshells of the M shell on the $K\alpha L^0$ transition energies has been examined. It is, however, interesting to know how removing electrons from the M shell influences the structure of the particular types of transitions for the $K\alpha L^n$ satellite lines.

A sample study has been carried out on palladium's $(1s2p)^{-1} \rightarrow 2p^{-2}$ transition type. To overcome increasing of the number of states, only removing all electrons from the M shell has been considered. On the other hand, removing all M-shell electrons enables to estimate the upper bound of the effect of M-shell holes on the energies of the transitions.

As shown [see Fig. 2(d)], removing M shell results in shifting the lines by about 3 hartree. The structures of the groups of lines are very similar though distance between the corresponding $K\alpha_1 L^1$ and $K\alpha_2 L^1$ lines in-

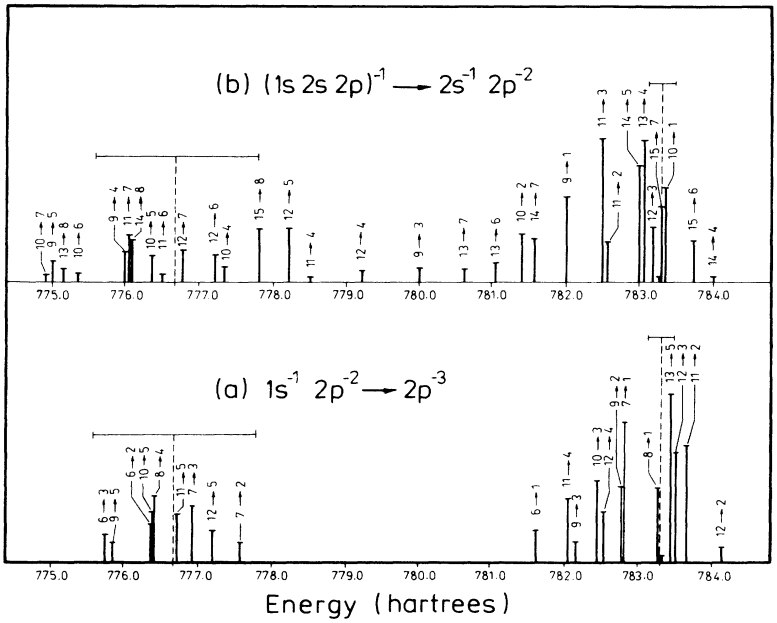

FIG. 4. Calculated line positions (in hartrees) with their relative intensities, to the same scale, shown in the stick spectrum for $K\alpha L^2$ satellite transitions of the types (a) $1s^{-1}2p^{-2} \rightarrow 2p^{-3}$, (b) $(1s2s2p)^{-1} \rightarrow 2s^{-1}2p^{-2}$. The recent measured (Ref. 26) experimental positions of the appropriate $K\alpha L^2$ satellite lines are shown as dotted lines.

creases by 0.2 hartree. Note that all these effects, even more enhanced, are observed when comparing the groups of transitions for which the initial states differ by the absence of $2s$ subshell (see Fig. 2 and Table IX).

IV. CONCLUSIONS

The test studies have shown that MCDF-AL version of MCDF calculations with the inclusion of the transverse (Breit) interaction, self-energy, and vacuum polarization corrections is accurate enough to reproduce very well the experimental positions and intensity ratios of the principal $K\alpha$ ($K\alpha L^0$) lines. The examination of the effect of removing subshells of the M shell on the $K\alpha L^0$ lines indicates that except for the case of holmium the effect of removing a particular subshell increases in the order $3d < 3s < 3p$. In the case of $3d$ this effect is relatively

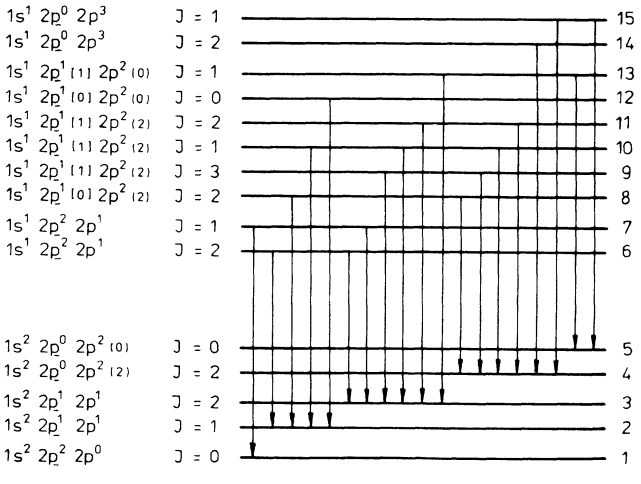

FIG. 5. Transition diagram for $K\alpha L^3$ satellite lines of the type $1s^{-1}2p^{-3} \rightarrow 2p^{-4}$.

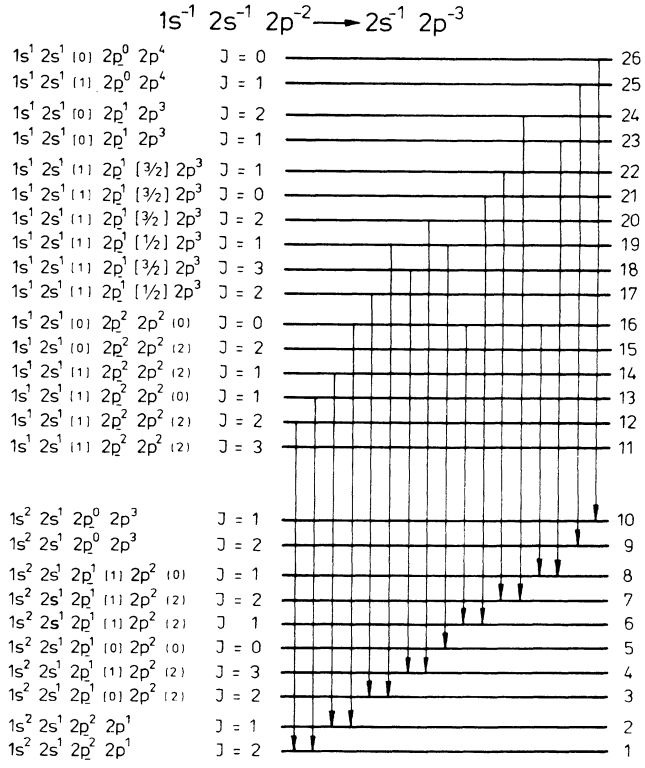

FIG. 6. Transition diagram for $K\alpha L^3$ satellite lines of the type $1s^{-1}2s^{-1}2p^{-2} \rightarrow 2s^{-1}2p^{-3}$.

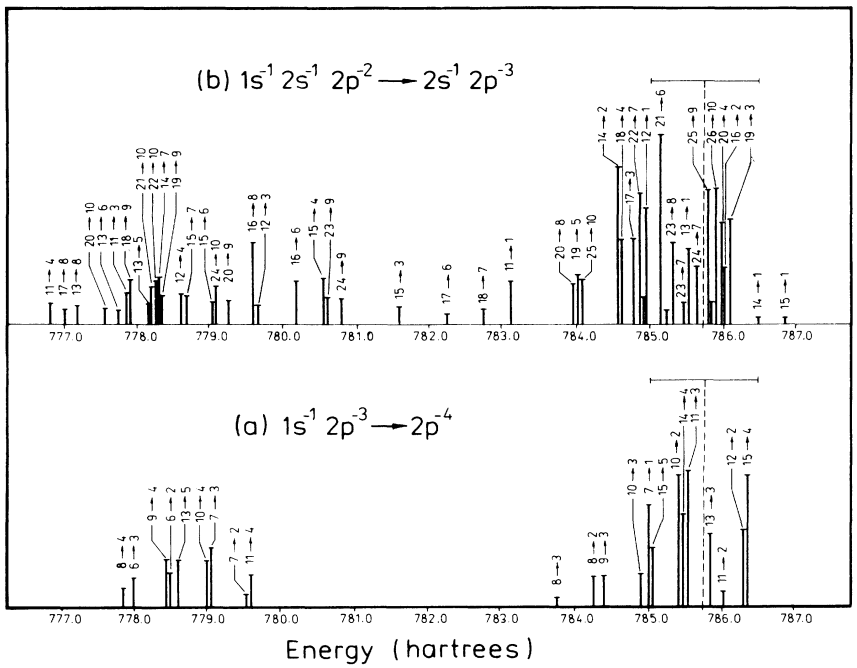

FIG. 7. Calculated line positions (in hartrees) with their relative intensities, to the same scale, shown in the stick spectrum for $K\alpha L^3$ satellite transitions of the types (a) $1s^{-1}2p^{-3}\rightarrow 2p^{-4}$, (b) $1s^{-1}2s^{-1}2p^{-2}\rightarrow 2s^{-1}2p^{-3}$. The recently measured (Ref. 26) experimental position of the $K\alpha_1 L^3$ satellite lines is shown as dotted line.

small and transition energy can be shifted either towards higher or lower values, while in the remaining cases the shift is large and always towards higher values. It can also be observed that the shift effects are not additive and remarkably increase with the atomic number.

Considerable attention has been paid to the analysis of the structure of the groups of lines corresponding to various types of transitions for the $K\alpha L^n$ satellites. On the basis of the calculations for palladium some general conclusions can be drawn.

First, in the case of each type of transition two groups of lines are observed, from which those of lower energies can be attributed to $K\alpha_2 L^n$ and those of higher energies to $K\alpha_1 L^n$. Second, the number of possible transitions increases rapidly with increasing the number of states possible for the given initial and final configurations. At the same time the energy differences between neighboring lines decrease and the distribution of lines around $K\alpha_2 L^n$ and $K\alpha_1 L^n$ positions becomes broader, causing in the most complex case ($1s^{-1}2s^{-1}2p^{-2}\rightarrow 2s^{-1}2p^{-3}$ of the $K\alpha L^3$ satellite) overlapping of those two groups of lines. Third, removing even a small number of electrons from the L shell causes, in most cases, a dramatic increase of the number of lines. Fourth, in most cases the energy differences between neighboring lines are much smaller than the natural linewidth [with the exception of $1s^{-1}2s^{-2}\rightarrow 2s^{-2}2p^{-1}$ and $(1s2s)^{-1}\rightarrow(2s2p)^{-1}$ cases]. Fifth, due to conclusion mentioned above, the overlapping of lines will simply prohibit a full resolution of the spectra. In general, the $K\alpha L^n$ satellite lines could be experimentally observed merely as some broad bands centered around $K\alpha_2 L^n$ and $K\alpha_1 L^n$ positions.

The comparison of the theoretical and experimental positions of the $K\alpha L^n$ satellite lines reveals that for all the types of transitions the "average" theoretical values are close to experiment while the best agreement is achieved for the type of $1s^{-1}2p^{-n}\rightarrow 2p^{-(n+1)}$ transitions. This is probably due to the Coster-Kronig transitions, which account for the rapid conversion of $2s$ hole states into $2p$ hole states. Therefore the important conclusion can be drawn that the $1s^{-1}2p^{-n}\rightarrow 2p^{-(n+1)}$ transitions give the dominant contribution to the $K\alpha L^n$ satellite lines in the x-ray spectra for heavy atoms. Moreover, it has been noted that for "average $K\alpha L^n$" the $K\alpha_2/K\alpha_1$ probability ratio remarkably decreases with increasing n and always strongly decreases with increasing number of $2p$ holes.

Besides, we must not forget that the $K\alpha L^n$ satellite lines corresponding to various n are overlapped, and moreover, that there are also various holes in the M and N shells, which makes the structure of the spectrum much more complex than it was presented in this work. Therefore, given a certain experimentally observed band, one can hardly realize the whole complexity of its structure.

The author believes that the results of his analysis will be helpful in a better understanding of the structure of the $K\alpha L^n$ satellite lines in x-ray spectra of heavy atoms and, moreover, will enable constructing different theoretical spectra for palladium. Clearly, to construct the particular theoretical $K\alpha L^n$ spectrum of palladium from the results of the present calculations some more information is required about the relative intensity ratios of various $K\alpha L^n$ satellites, the probabilities of creating the particu-

TABLE IX. Comparison of the theoretical and experimental positions of $K\alpha L^n$ satellite lines (in hartrees). The uncertainties of experimental results are marked in parentheses.

$K\alpha L^n$ satellite	$K\alpha_1 L^n$ E[a]	ΔE[b]	$K\alpha_2 L^n$ E	ΔE	$K\alpha_2/K\alpha_1$ prob. ratio
Theor. $K\alpha L^0$	778.280		772.520		0.5297
Expt. $K\alpha L^0$	778.242[c] (0.004)		772.472[c] (0.004)		0.529[d]
	778.514[e] (0.015)	0.272[f] (0.019)	772.714[e] (0.029)	0.242[f] (0.033)	
Theor. $K\alpha L^1$[g]					
$(1s2s)^{-1}$	780.245	1.965	774.613	2.094	0.5269
$(1s2p)^{-1}$	780.585	2.305	774.513	1.994	0.4902
Av. $K\alpha L^1$[h]	780.491	2.221	774.543	2.023	0.5004
Expt. $K\alpha L^1$	780.81 (0.07)	2.30 (0.09)	774.71 (0.11)	2.00 (0.14)	
Theor. $K\alpha L^2$[g]					
$1s^{-1}2s^{-2}$	782.419	4.139	776.476	3.956	0.5287
$(1s2s2p)^{-1}$	782.574	4.294	776.676	4.156	0.4917
$1s^{-1}2p^{-2}$	782.932	4.652	776.537	4.017	0.4553
Av. $K\alpha L^2$[h]	782.748	4.468	776.604	4.084	0.4745
Expt. $K\alpha L^2$	783.31 (0.18)	4.80 (0.20)	776.7 (1.1)	4.0 (1.1)	
Theor. $K\alpha L^3$[g]					
$1s^{-1}2s^{-2}2p^{-1}$	784.792	6.512	778.531	6.011	0.4893
$1s^{-1}2s^{-1}2p^{-2}$	784.973	6.693	778.767	6.247	0.4704
$1s^{-1}2p^{-3}$	785.418	7.138	778.680	6.160	0.4267
Av. $K\alpha L^3$[h]	785.078	6.798	778.708	6.188	0.4601
Expt. $K\alpha L^3$	785.74 (0.73)	7.22 (0.75)	n.a.[i]	n.a.	

[a]"Average" theoretical (see text) and experimental positions of $K\alpha L^n$ satellite lines.
[b]"Relative" positions of $K\alpha L^n$ satellites; $\Delta E = E(K\alpha L^n) - E(K\alpha L^0)$.
[c]Bearden (Ref. 25).
[d]Salem *et al.* (Ref. 28).
[e]Rymuza *et al.* (Ref. 26).
[f]Experimentally measured effect of removing electrons from M shell [the difference between results of Rymuza *et al.* (Ref. 26) and Bearden (Ref. 25)].
[g]The theoretical results for particular types of transitions of each $K\alpha L^n$ satellite (only the initial configurations of the corresponding types of transitions are indicated in table).
[h]The average of results for particular types of transitions weighted with the probabilities of creating appropriate initial configurations (the influence of the Coster-Kronig transitions has been neglected).
[i]The experimental values are not available since the $K\alpha_2 L^3$ band is fully covered by a strong $K\alpha_1 L^0$ principal band.

lar type of initial configurations for each satellite and a quantitative influence of the Coster-Kronig transitions.

To accurately reproduce both the position of satellites and the shape of the experimental spectrum it is necessary to perform a detailed investigation in which various M-shell holes will be taken into account together with L-shell holes (the $K\alpha L^n M^r$ lines). Preliminary investigations are already in progress.

ACKNOWLEDGMENTS

The author would like to thank Professor I. P. Grant for enabling the Institute of Physics of the Nicholas Copernicus University to use his MCDF program package. This work has been supported by the Polish Central Project of Fundamental Research Grant No. CPBP-01.06.

[1]E. U. Condon and G. H. Shortley, *The Theory of Atomic Spectra* (Cambridge University Press, New York, 1953).
[2]L. G. Parratt, Phys. Rev. B **49**, 502 (1936); **50**, 1 (1936).
[3]*Atomic Inner-Shell Physics,* edited by B. Crasemann (Plenum, New York, 1985), and references therein.
[4]B. Perny, J.-Cl. Dousse, M. Gasser, J. Kern, Ch. Rheme, P. Rymuza, and Z. Sujkowski, Phys. Rev. A **36**, 2120 (1987).
[5]R. L. Kauffman, J. H. McGuire, P. Richard, and C. F. Moore,

Phys. Rev. A **8**, 1233 (1973).
[6]A. R. Knudson, D. J. Nagel, P. G. Burkhalter, and K. L. Dunning, Phys. Rev. Lett. **26**, 1149 (1971).
[7]D. Burch, P. Richard, and R. L. Blake, Phys. Rev. Lett. **26**, 1355 (1971).
[8]D. G. McCrary and P. Richard, Phys. Rev. A **5**, 1249 (1972).
[9]F. A. Gianturco, E. Semprini, and F. Stefani, Physica **80C**, 613 (1975).
[10]D. L. Matthews, B. M. Johnson, and C. F. Moore, At. Data Nucl. Data Tables **15**, 41 (1975).
[11]K. W. Hill, B. L. Doyle, S. M. Shafroth, D. H. Madison, and R. D. Deslattes, Phys. Rev. A **13**, 1334 (1976).
[12]I. P. Grant, Int. J. Quantum Chem. **25**, 23 (1984).
[13]W. J. Kuhn and B. L. Scott, Phys. Rev. A **34**, 1125 (1986).
[14]B. L. Scott, Phys. Rev. A **34**, 4438 (1986).
[15]W. Uchal, C. W. Nestor, Jr., S. Raman, and C. R. Vane, At. Data Nucl. Data Tables **34**, 301 (1986).
[16]R. J. Maurer and R. L. Watson, At. Data Nucl. Data Tables **34**, 185 (1986).
[17]I. P. Grant, B. J. McKenzie, P. H. Norrington, D. F. Mayers, and N. C. Pyper, Comput. Phys. Commun. **21**, 207 (1980).
[18]B. J. McKenzie, I. P. Grant, and P. H. Norrington, Comput. Phys. Commun. **21**, 233 (1980).
[19]I. P. Grant and B. J. McKenzie, J. Phys. B **13**, 2671 (1980).
[20]J. Hata and I. P. Grant, J. Phys. B **16**, 3713 (1983).
[21]J. Karwowski and J. Styszyński, Int. J. Quantum Chem. **28**, 27 (1985).
[22]I. P. Grant, J. Phys. B **7**, 1458 (1974).
[23]L. W. Fullerton and G. A. Rinker, Phys. Rev. A **13**, 1283 (1976).
[24]P. J. Mohr, Ann. Phys. (N.Y.) **88**, 52 (1974); Phys. Rev. Lett. **34**, 1050 (1975); Phys. Rev. A **26**, 2338 (1982).
[25]J. A. Bearden, Rev. Mod. Phys. **39**, 78 (1967).
[26]P. Rymuza, Z. Sujkowski, M. Carlen, J.-Cl. Dousse, M. Gasser, J. Kern, B. Perny, and Ch. Rheme (unpublished).
[27]S. I. Salem and P. L. Lee, At. Data Nucl. Data Tables **18**, 233 (1976).
[28]S. I. Salem, S. L. Panossian, and R. A. Krause, At. Data Nucl. Data Tables **14**, 91 (1974).
[29]E. J. McGuire, Phys. Rev. A **2**, 273 (1970); **3**, 587 (1971); **3**, 1801 (1971).